

Elastohydrodynamics of Concentrated Suspension with Generalized Newtonian Fluid Medium

Sang-Yoon Kang[†]

Department of Chemical Engineering, Korea Advanced Institute of Science and Technology,
Daejeon 305-701, Korea

(Received 31 October 2001 • accepted 16 January 2002)

Abstract—Lubrication theory is applied to compute the deformation of two approaching particles suspended in a Generalized Newtonian fluid with linear elastic theory estimating deformation and force on the particles with respect to deformability δ . The relative viscosity of concentrated suspension with deformable particles in a Generalized Newtonian fluid is obtained for a simple cubic array configuration by using the results of deformation and force for two particles. Since the deformation of particles generates the freedom of moving particles geometrically, the suspension with deformable particles shows shear thinning behavior.

Key words: Lubrication Theory, Hertz Contact Theory, Deformability, Generalized Newtonian Fluid, Relative Viscosity

INTRODUCTION

The rheology of highly concentrated blends has been studied experimentally by many investigators [Munstedt, 1981; Ellul et al., 1995; Abdou-Sabet et al., 1996; Araki and White, 1998; Kim and Chun, 1999; Moon et al., 2001] to understand the behavior of blend during the process. However, a prominent barrier to the use of polymer blends and composite materials is the lack of adequate models that capture the complex interaction between microstructure and rheology of these materials during processing. In determining the rheological property of polymer blends, the most significant features are hydrodynamic interaction between neighboring particles and deformation of particles. Thus, we would like to focus on those two phenomena to establish a useful model of suspension rheology with deformable particles.

Many investigators have been working on understanding the hydrodynamic interactions of highly concentrated systems of hard spheres. Since the hydrodynamic interactions between neighboring particles are governed by lubrication force, the relative viscosity of concentrated suspension with Newtonian fluid medium was developed from the rate of energy dissipation for two nearly touching spherical rigid particles taking the spherical cell around particles [Frankel and Acrivos, 1967]. Jarzebski [1981] and Tanaka et al. [1980] extended to non-Newtonian fluid medium using the same method. The stress between two particles was approximated as pressure distribution by Tanaka et al. [1980] while stress was estimated as the shear contribution of deformation tensor in second invariant by Jarzebski [1981] claiming the more importance of elongation. Jarzebski [1981] showed that the relative viscosity was lowered as shear index n is decreased owing to the extensional motion of fluid at the surface of particles. Recently, the rheological behavior of concentrated suspension with rigid particles in Newtonian fluid was examined with Stokesian dynamic simulations considering only lubri-

cation force as the interactions of particles [Ball and Melrose, 1995, 1997; Catherall et al., 2000] as well as were investigated experimentally by Lee et al. [1999] and So et al. [2001] showing the shear thickening behavior due to clustering of particles caused by lubrication force.

Local volume averaging [Batchelor, 1970] was used for averaging stresslet so as to estimate the concentrated suspension viscosity for a static periodic configuration instead of spherical cell approximating the stresslet of suspension from lubrication force and vector connecting center of two neighboring rigid particles [van den Brule and Jongschaap, 1991].

Suspended particles such as rubber or conducting drop can be deformed by external force, e.g. hydrodynamic interaction between particles or electric field [Ha and Yang, 2000]. The deformation due to short range hydrodynamic force has been estimated for elastic particles in Newtonian fluid medium by Christensen [1970] and Davis et al. [1986] combined with Hertz contact theory [Landau and Lifshitz, 1986]. Different than the suspension of hard spheres, rheologically shear thinning behavior is observed for the suspension of deformable particles since deformation allows the mobility of particles to increase geometrically [Loewenberg and Hinch, 1996].

In this paper we employ the volume averaging method to understand the rheological behavior of concentrated suspension with deformable particles suspended in Newtonian as well as in non-Newtonian fluid. However, it may be desirable to accomplish the dynamic simulation of deformable particles to predict the relative viscosity; the computational time is so tremendous that it will be worked on in the next paper. A periodic configuration is therefore used in estimating the relative viscosity of suspension with deformable particles.

In the following section, lubrication force and deformability between two rubber particles are derived before calculating the relative viscosity of suspension along with the brief description of numerical scheme. Then the results of numerical computation for two deformable are presented for various shear indices and deformabilities δ . In the final section the relative viscosity of deformable par-

[†]To whom correspondence should be addressed.
E-mail: kangsa@mail.kaist.ac.kr

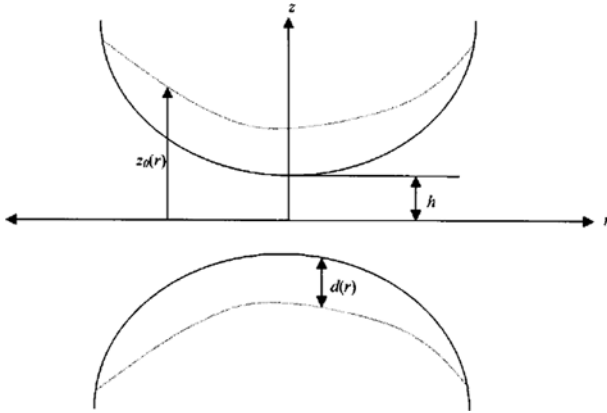


Fig. 1. Schematic of two deformable particles.

ticles is estimated from the results of previous section.

LUBRICATION THEORY AND DEFORMABILITY

Two spherical elastic particles with radius a are approaching each other as shown in Fig. 1. As they get closer, the pressure between them is increased inducing the stronger stress on the surface of particles. The curvature of deformed particle is approximately expressed as

$$z(r, t) = h(t) + \frac{r^2}{2a} + d(r, t) \quad (1)$$

Here $h(t)$ is the hypothetical distance of two deformable particles on the line connecting the centers of particles shown as a solid line. In other words, it is the distance of two particles assuming no deformation occurs. For deformable particles, variable $d(r, t)$ is determined by its elastic properties, e.g. Poisson ratio ν and Young's modulus E . The total particle deformation d in narrow gaps between two approaching rubber particles suspended in Generalized Newtonian fluid is evaluated as follows with the Hertz contact theory of linear elasticity.

$$\begin{aligned} \Delta = \frac{d}{h} &= \delta J_1(R, n, \delta), \quad R = \frac{r}{(ha)^2} \\ J_1(R, n, \delta) &= 2^{n+1} \left(\frac{2n+1}{2n} \right)^n \left[\int_0^\infty \frac{R^m}{[1+R'^2/2 + \Delta(R', \delta)]^{1+2n}} dR' \right] \phi(R, \xi) d\xi \end{aligned} \quad (2)$$

where δ is the *deformability* of particle and is defined as

$$\delta = \frac{2^{(n+2)/2} \theta K u^a a^{(n+2)/2}}{h^{3(n+2)/2}}, \quad \theta = \frac{2(1-\nu^2)}{\pi E} \quad (3)$$

where K is the consistent coefficient of power law fluid, n is the shear index and u is the relative velocity of two particles. The function ϕ in J_1 involves a complete elliptic integral of first kind and is given as follows.

$$\phi(R, \xi) = \frac{\xi}{\xi + R} \Im \left[\frac{4\xi R}{(\xi + R)^2} \right] \quad (4)$$

The bracketed integration term in (2) corresponds to the stress distribution over the surface at time t , which is determined from the hydrodynamic interaction of two particles. As seen in (2), the combi-

nation of two physical phenomena, i.e. lubrication effect and elastic properties, allows us evaluate the deformation. By the coupling of continuity and momentum equation, the well-known lubrication equation for the gap of two particles is expressed as

$$\frac{\partial z}{\partial t} = \frac{1}{12 \mu r} \frac{\partial}{\partial r} \left[r z^3 \frac{\partial p}{\partial r} \right] \quad (5)$$

Since the deformation $d(r, t)$ is incorporated in curvature equation as (1), deformation owing to elasticity and lubrication force can be combined into the equation through (5). The force F on the two deformable particles is estimated from the stress distribution obtained from (5).

$$\begin{aligned} F &= \int_0^\infty \sigma_{zz} (2\pi) r dr = 2\pi K u^a h^{\frac{1-3n}{2}} a^{\frac{3+n}{2}} \left(\frac{1}{2} \right)^{\frac{1-n}{2}} J_2(n, \delta) \\ J_2(n, \delta) &= \left(\frac{2n+1}{2n} \right)^n \int_0^\infty \left[\int_0^\infty \frac{R^m}{[1+R'^2/2 + \Delta(R', \delta)]^{1+2n}} dR' \right] R dR \end{aligned} \quad (6)$$

In evaluating normal stress σ_{zz} , only pressure P is included since the magnitude of gradient of axial direction velocity w with respect to z is much smaller, e.g. $P \sim O(h^{-2})$ and $(\partial w / \partial z) \sim O(h^{-1})$ for Newtonian fluid. The force equation is reduced to (7) with $J_2 = 3/4$ when the particles are rigid and fluid medium is Newtonian, implying that the magnitude of force is strongly dependent on the gap size h .

$$F_{rigid} = \frac{3}{2} \pi \mu a^2 \frac{u}{h} \quad (7)$$

A complete solution of the lubrication equation coupled with elasticity theory can be evaluated by numerical methods, e.g. finite difference, finite element etc., as a function of time. In this work, the computation of instant deformation and force acting on the surface of deformed particles is enough to predict the relative viscosity for a given configuration. Therefore, we calculated the $d(r)$ with the pressure distribution obtained from two approaching rigid spheres as a first step, considering the left side of (5) as the relative velocity of two particles. Consecutively, the newly obtained pressure distribution $P(r)$ from the previous step is used for the evaluation of $d(r)$. This procedure is repeated until $d(r)$ and P are converged. Once numerically converged $d(r)$ and P is computed, the lubrication force written in (6) is estimated numerically. Romberg integration is used to calculate J_1 and J_2 precisely, changing variables to avoid the singularity due to integrand.

SIMULATION RESULTS

The distribution of particle curvature, integration J_2 and lubrication forces are computed for Newtonian fluid and a non-Newtonian fluid satisfying power law with shear index as 0.5, varying deformability. In Figs. 2 and 4, surface curvature in the radial direction is plotted for several elastic parameters along with the pressure distributions between two particles shown in Fig. 3 and 5. More deformation occurs as deformability increases. About 40% of gap size h is deformed for $\delta=0.1$, whereas almost no deformation is observed for $\delta \approx 10^{-4}$ as seen in Fig. 2. It is also shown that the most deformation occurs at $R=0$, where the highest stress is applied, and the extent of deformation is reduced as one moves along the radial direction. The pressure distribution plots confirm this trend showing that the pressures at the center are distributed discretely while

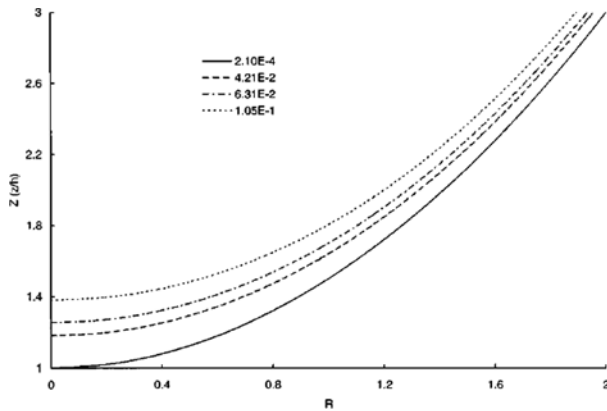


Fig. 2. The distribution of particle curvature with Newtonian fluid medium. The lines have different deformability δ as shown in legend.

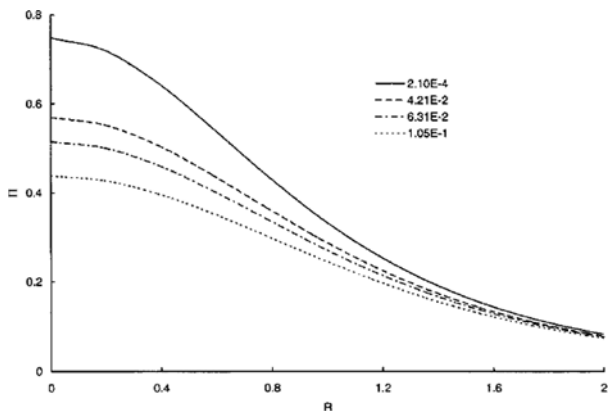


Fig. 3. Pressure distribution curves along the surface of deformable particle suspended in Newtonian fluid for different deformability δ . Scaled pressure Π is defined as $\text{Ph}^2/\mu a$.

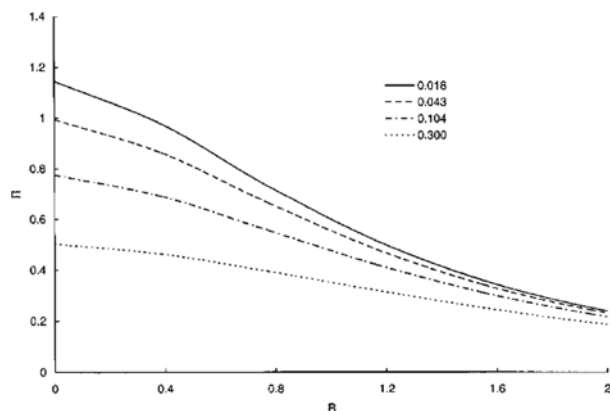


Fig. 5. Pressure distribution curves along the surface of deformable particle suspended in non-Newtonian fluid with shear index as 0.5 for different deformability δ . Scaled pressure Π is defined as $\text{Ph}^{1.25}/\text{Ku}^{0.5} a^{0.75}$.

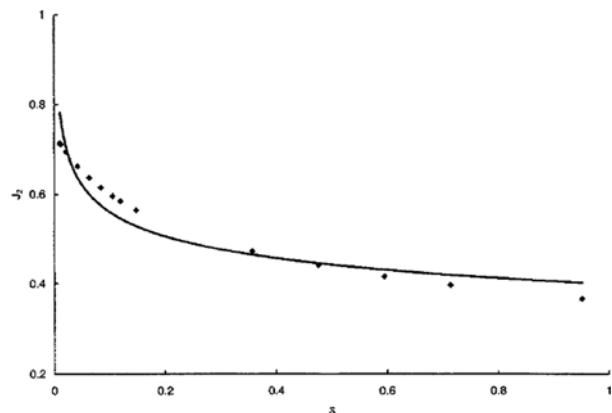


Fig. 6. J_2 with respect to deformability δ for Newtonian fluid medium. Solid line is the trend line expressed with power law.

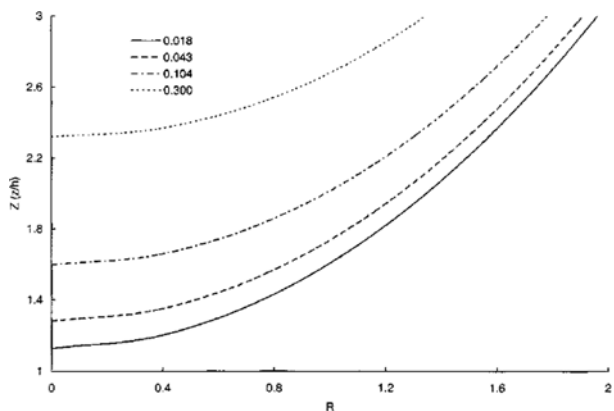


Fig. 4. The distribution of particle curvature with non-Newtonian fluid medium with shear index as 0.5. The lines have different deformability δ as shown in legend.

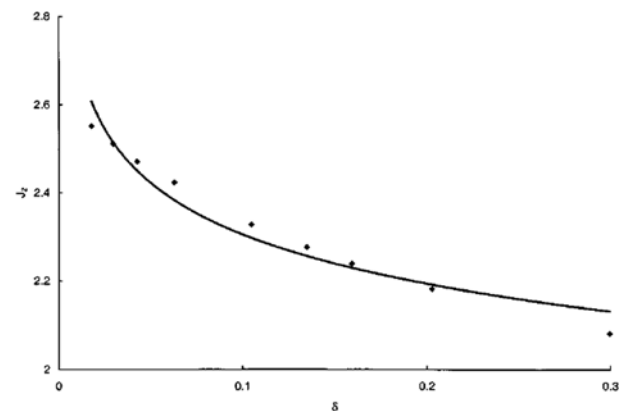


Fig. 7. J_2 with respect to deformability δ for non-Newtonian fluid medium with shear index as 0.5. Solid line is the trend line expressed with power law.

they are converged to almost same as R increases. Note that the pressure is decreased as the deformation increases and deformability increases. The stress acting on the surface of particles is already relaxed into the deformation resulting in letting gap size bigger. The pressure is therefore lowered as seen in Figs. 3 and 5 owing to high

deformation of surface.

The most significant part of lubrication force is the computation of integration J_2 as shown in Figs. 6 and 7. The analytical J_2 for a rigid body in a Newtonian fluid is 0.75 as seen in (7) implicitly. Since the calculated force is used in predicting relative viscosity, the cor-

Table 1. Power and coefficient for the trend line of J_2 in expressing $J_2 = C\delta^{-m}$. C_0 is the value of J_2 and $m=0$ when particles are rigid

n	1	0.5
m	0.147	0.072
C	0.399	1.955
C_0	0.750	2.626

relation function between J_2 and deformability is necessary on the basis of simulation results to obtain the proper rheological relationship of suspension with deformable particles such as polymer blends. As deformability increases, J_2 is decreased following a power law. The power and coefficients are listed in Table 1. The solid lines in Figs. 6 and 7 represent trend lines by power laws. Lubrication force is proportional to $h^{-0.85}$ for deformable particles in Newtonian fluid and is $h^{-0.12}$ for deformable particles in non-Newtonian power law fluid with shear index as 0.5 while it is h^{-1} and $h^{-0.25}$ respectively for rigid particles. The dependency on h is shown slightly weaker for deformable particles because force depends on h as well as deformed curvature of surface in integration J_2 .

It is worthwhile to see the effect of deformation on the lubrication force by a force ratio Φ defined as the ratio of force with deformable particles and force with rigid particles. As Φ departs from unity, the force acting on the surface of deformable particles is less than that on the rigid particles. In other words, the deformation occurring generates more space between two particles resulting in less pressure in the gap. Since the deformability δ gets bigger and bigger, the force ratio Φ is decreased as shown in Fig. 8. For the non-Newtonian fluid medium with $n=0.5$, Φ is changed about 15%, whereas it is varied more than 25% for a Newtonian fluid. It is noted that the particles in Newtonian fluid medium are more impacted by deformation. Non-Newtonian fluids following the power law intrinsically have extensional motion during the process, which may create sliding at the surface and in turn produce comparatively small deformation.

RELATIVE VISCOSITY

The suspension viscosity has very different flow behavior with

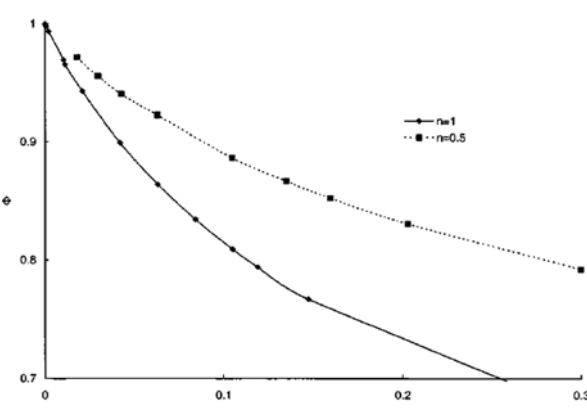


Fig. 8. The ratio of force between deformable particle and rigid particle, Φ , as a function of deformability.

that of fluid medium since the suspending particles' interactions contribute very much to the bulk stress of suspension. In particular, the pair interactions due to lubrication force between particles are most significant at high particle volume fraction. Therefore, relative viscosity, as defined in (8), varies depending on the volume fraction of particles, applied mean flow, viscosity of fluid medium, properties of suspending particles etc.

$$\text{relative viscosity } (\mu_r) = \frac{\text{viscosity of suspension } \mu}{\text{viscosity of fluid medium } \mu_m}. \quad (8)$$

Van den Brule and Jongschaap [1991] approached the relative viscosity of a Newtonian fluid by using stress expression for suspension proposed by Batchelor [1970]. As seen in (9) the suspension stress T_{ij} for the overall suspension volume V has the contribution of fluid medium and that of particle interactions t_{ij} , so called as particle phase stress, after very small magnitude terms are neglected. P is the pressure, $T_{ij(m)}$ is the deviatoric stress tensor of fluid medium and V_0 is the volume of suspended particles.

$$T_{ij} = \frac{1}{V} \int_{V - \sum V_i} (-P\delta_{ij} + T_{ij(m)}) dV + \frac{1}{V} \sum_i \int_{V_i} t_{ij} dV \quad (9)$$

In concentrated suspension the lubrication force between particles is most important and screens the long-range hydrodynamic forces effectively. Only the short-range interaction is thus considered in the suspension stress to change the second term of (9) for a given configuration, e.g., simple cubic array or face centered array etc. The stress due to particles' pair interaction in a concentrated system is therefore computed with

$$T_{ij}^P = \frac{1}{V} \sum_i F_i^{\alpha\beta} r_i^{\alpha\beta} \quad (10)$$

where $F_i^{\alpha\beta}$ is the lubrication force between particle α and β , and $r_i^{\alpha\beta}$ is the vector connecting the center to center of particles α and β . Thus, lubrication force for a pair particle is used, in the previous section, to predict the relative viscosity of suspension with deformable particles.

Including the deformation effects which were presented only in evaluating the integral J_2 , the lubrication force can be rewritten differently incorporating the approximate equation of $J_2(n, \varepsilon)$ into (6). Therefore, the force between two particles in Generalized Newtonian fluids is

$$F_i = C_1 \theta^{-m} K^{1-m} a^{(n(1-m)-2m+3)/2} h^{(3n(m-1)+2m+1)/2} u^{n-mm} e_i, \\ C_1 = 2^{(1+n-mm-2m)/2} \pi C. \quad (11)$$

This expression will be used in calculation of a particle's contribution to bulk stress in the following. Here m is the power of elastic parameter, C is the coefficient of power and e is the unit vector. The values of C and m can be found as listed in Table 1 from Figs. 6 and 7. Note that $C=0.75$, $m=0$ for rigid particles in Newtonian fluid and $C \approx 2.626$, $m=0$ for rigid particles in non-Newtonian fluid with shear index as 0.5. The relative velocity u can be expressed with distance r , macroscopic velocity gradient L and bulk rate of strain tensor D as

$$u = r L \cdot e = r (D : e e) e. \quad (12)$$

Thus, particle phase stress (10) can be written with D after the above velocity relation is substituted into (12).

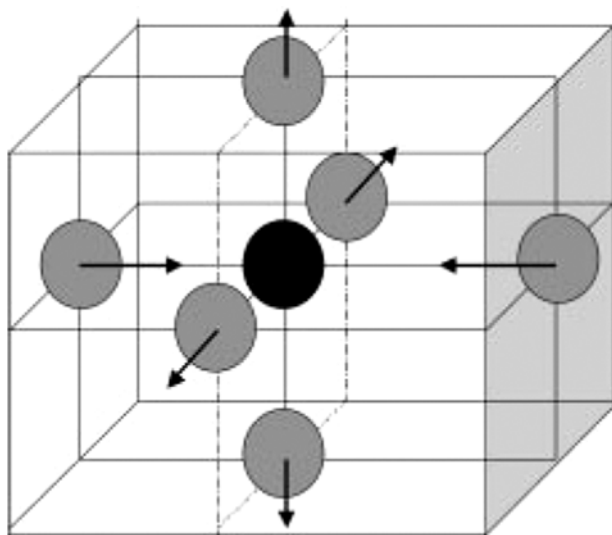


Fig. 9. Simple cubic array of particles arranged with the principal axes of deformation tensor. The black sphere is the reference to other surrounding particles presented as semi-transparent.

$$F_i r_i = C_1 \theta^{-m} K^{1-m} a^{(n(1-m)-2m+3)\gamma/2} h^{(3n(m-1)+2m+1)\gamma/2} (D_{ik} e_k e_l)^{n-m} e_i r^{1+n(1-m)} e_j \quad (13)$$

For the particle in a simple cubic array, the orientation of packed array is arranged with principal axes of the rate of strain tensor as seen in Fig. 9, saying that the *pure shearing* deformation of cubic array is considered here. In a given unit volume V , six particles surround the reference particle as shown black in the center of the box. Writing (13) for an approaching particle,

$$F_i r_i = C_1 \theta^{-m} K^{1-m} a^{(n(1-m)-2m+3)\gamma/2} h^{(3n(m-1)+2m+1)\gamma/2} r^{1+n(1-m)} D_{11}^{n-m} e_1 e_1. \quad (14)$$

Similarly, other neighboring particles contribute to the overall stress tensor. Summing up all the contributions of neighboring particles to estimate the stress tensor of a suspension aligned in a cubic array, (9) is simplified to (15) due to dominating pure shearing motion when instantaneous configuration of neighbors is known.

$$T_{11} = 2^{(n+1)\gamma/2} K \gamma^n + \frac{1}{2} n \sum F_i r_i, \quad \gamma = D_{11} \quad n : \text{number density}$$

$$T_{11} = 2^{(n+1)\gamma/2} K \gamma^n [1 + 2^{-6\gamma/2} C_1 (K \theta)^{-m} a^{(n(1-m)-2m+3)\gamma/2} h^{(3n(m-1)+2m+1)\gamma/2} r^{1+n(1-m)} n \gamma^{-m}] \quad (15)$$

The distance r and number density n can be approximated as $2a$ and $1/r^3$ since the particles are so closely packed. Consequently, the relative viscosity is expressed as

$$\mu_r = 1 + C_2 \Lambda \left(\frac{a}{h} \right)^{(3n(1-m)-2m-1)\gamma/2}, \quad C_2 = 2^{(n-2m-5)\gamma/2} C_1, \quad \Lambda = K \theta \gamma^n$$

$$= 1 + C_2 \Lambda^{-m} \left[\frac{(\phi/\phi_m)^{1/3}}{2(1-(\phi/\phi_m)^{1/3})} \right]^{(3n(1-m)-2m-1)\gamma/2} \quad (16)$$

ϕ_m is the maximum volume fraction of arrangement. For the simple cubic array it is $\pi/6=0.5236$ and is $\pi/3\sqrt{2}=0.7405$ for hexagonal arrangement. The coefficient of large bracket is changed for the different configurations of suspension, depending on how many particles approach together. As for the rigid particles, the coefficient of bracket is $3\pi/16$ for the simple cubic array and it is changed to $3\pi\sqrt{2}/16$ for the hexagonal arrangement.

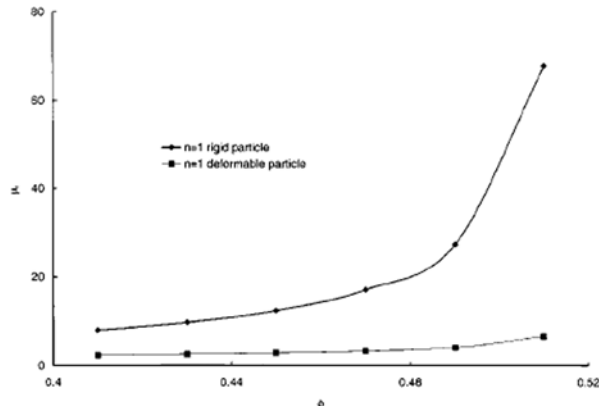


Fig. 10. The relative viscosity μ_r of deformable and rigid particles for Newtonian fluid medium for various volume fractions with $\Lambda=2$.

16 for the hexagonal arrangement [van den Brule, 1991]. The comparisons of effective viscosity of suspension between rigid particles and deformable particles is shown in Figs. 10 and 11 for the simple cubic array with Newtonian fluid medium as well as with non-Newtonian fluid with shear index as 0.5 varying volume fraction. Here m is taken as zero and C is taken as C_0 in Table 1. As discussed by

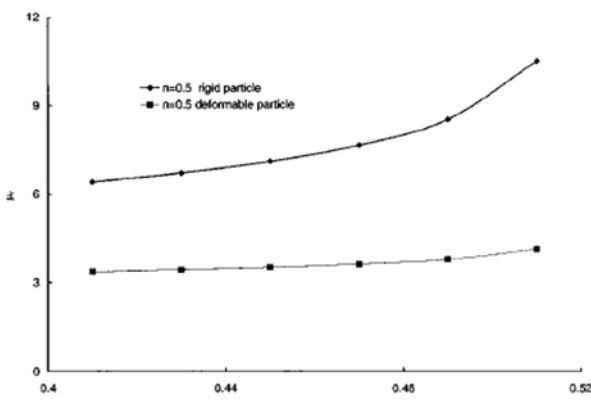


Fig. 11. The relative viscosity μ_r of deformable and rigid particles for non-Newtonian fluid medium with shear index as 0.5 for various volume fractions with $\Lambda=2$.

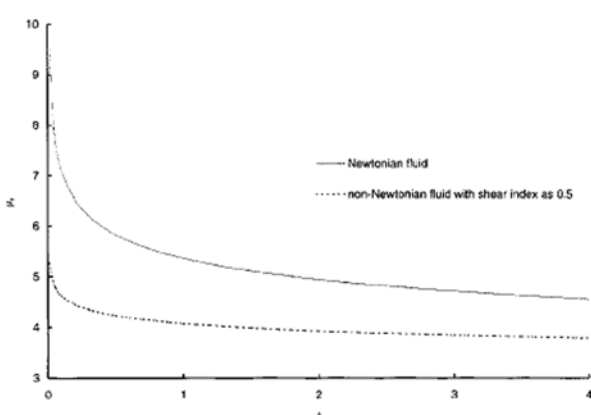


Fig. 12. The relative viscosity μ_r of deformable particles with respect to Λ at volume fraction = 0.5.

Jarzebski [1981], suspension of a Newtonian fluid has higher relative viscosity in a concentrated system because the suspension of non-Newtonian fluid satisfying the power law has extensional property at the surface of particle. The plots for deformable particles are obtained taking Λ as 2 for both fluid mediums, which is explicitly connected to deformability parameter δ . As seen in Fig. 8, Φ is changed less when the fluid medium is non-Newtonian, explaining that the relative viscosity is changed more for deformable particles in a Newtonian fluid. The deformation of particles gives room geometrically to move [Loewenberg and Hinch, 1996], when they meet together, decreasing the relative viscosity. Fig. 12 confirms that the deformation results in the decrease of relative viscosity as well as that shear thinning is observed in the presence of deformable particles. As shear rate increases, the approaching velocity is higher and higher to produce more deformation of particles so that prevents the sticking of particles and decreases the relative viscosity.

ACKNOWLEDGEMENT

S.-Y. Kang acknowledges the support for this work by BK21 program and thanks for discussion to Dr. Jayaraman in Michigan State University.

REFERENCES

Araki, T. and White, J. L., "Shear Viscosity of Rubber Modified Thermoplastics: Dynamically Vulcanized Thermoplastic Elastomers and ABS Resins at Low Stress," *Polymer Eng. Sci.*, **38**, 590 (1998).

Abdou-Sabet, S., Pudyak, R. C. and Rader, C. P., "Dynamically Vulcanized Thermoplastic Elastomers," *Rubber Chemistry and Technology*, **69**, 476 (1996).

Batchelor, G. K., "The Stress System in a Suspension of Force-Free Particles," *J. Fluid Mech.*, **41**, 545 (1970).

Ball, R. C. and Melrose, J. R., "The Pathological Behavior of Sheared Hard-Spheres with Hydrodynamic Interactions," *Europhysics Letters*, **32**, 535 (1995).

Ball, R. C. and Melrose, J. R., "A Simulation Technique for Many Spheres in Quasi-Static Motion Under Frame-invariant Pair Drag and Brownian Forces," *Physica A*, **247**, 444 (1997).

Catherall, A. A., Melrose, J. R. and Ball, R. C., "Shear Thickening and Order-Disorder Effects in Concentrated Colloids at High Shear Rates," *J. Rheol.*, **44**, 1 (2000).

Christensen, H., "Elastohydrodynamic Theory of Spherical Bodies in Normal Approach," *J. Lub. Tech.*, **92**, 145 (1970).

Davis, R. H., Serayssol, J. and Hinch, E. J., "The Elastohydrodynamic Collision of Two Spheres," *J. Fluid Mech.*, **163**, 479 (1986).

Frankel, N. A. and Acrivos, A., "On the Viscosity of a Concentrated Suspension of Solid Spheres," *Chem. Eng. Sci.*, **22**, 847 (1967).

Ha, J.-W. and Yang, S.-M., "Deformation and Breakup of Newtonian and Non-Newtonian Conducting Drops in an Electric Field," *J. Fluid Mech.*, **405**, 131 (2000).

Jarzebski, G. J., "On the Effective Viscosity of Pseudoplastic Suspensions," *Rheol. Acta*, **20**, 280 (1981).

Kim, S. W. and Chun, Y. H., "Barrier Property by Controlled Laminar Morphology of LLDPE/EVOH Blends," *Korean J. Chem. Eng.*, **16**, 511 (1999).

Landau, L. D. and Lifshitz, E. M., "Theory of Elasticity," 3rd ed. Pergamon Press, New York (1986).

Lee, J.-D., So, J.-H. and Yang, S.-M., "Rheological Behavior and Stability of Concentrated Silical Suspensions," *J. Rheology*, **43**, 1117 (1999).

Loewenberg, M. and Hinch, E. J., "Numerical Simulation of a Concentrated Emulsion in Shear Flow," *J. Fluid Mech.*, **321**, 395 (1996).

Moon, D. Y., Kwon, M. H. and Park, O. O., "Morphology Evolution in PS/LDPE Blends in a Twin Screw Extruder: Effects of Compatibilizer," *Korean J. Chem. Eng.*, **18**, 33 (2001).

Munstedt, H., "Rheology of Rubber Modified Polymer Melts," *Polym. Eng. Sci.*, **21**, 259 (1981).

So, J.-H., Yang, S.-M. and Hyun, J. C., "Microstructure Evolution and Rheological Responses of Hard Sphere Suspensions," *Chem. Eng. Sci.*, **56**, 2967 (2001).

Tanaka, N. and White, J. L., "A Cell Model Theory of the Shear Viscosity of a Concentrated Suspension of Interacting Spheres in Non-Newtonian Fluid," *J. Non-Newtonian Fluid Mech.*, **7**, 333 (1980).

Van den Brule, B. H. A. A. and Jongschaap, R. J. J., "Modeling of Concentrated Suspensions," *J. Statistical Physics*, **62**, 1225 (1991).